The Effect of Nano- and Micro-Fillers on the Strength and Toughness of PIR Foams Obtained From Renewable Resources

Janis Andersons[1,*], Ugis Cabulis[2], Uldis Stirna[2]

[1] Institute of Polymer Mechanics, University of Latvia, Riga LV-1006, Latvia
[2] Latvian State Institute of Wood Chemistry, Riga LV-1006, Latvia
* Corresponding author: janis.andersons@pmi.lv

Abstract Low-density rigid polyisocyanurate (PIR) foams obtained from renewable resources (with the polyol system comprising up to 80% of rapeseed oil esters) have been produced and tested for strength and fracture toughness in a range of foam density of importance for practical applications. In order to enhance the mechanical characteristics of the foams, the effect of several nano- and micro-fillers has been investigated experimentally. It is demonstrated that nano-fillers, such as organically modified nanoclays, carbon nanotubes, ZnO nanoparticles, increase both the strength and toughness of the foams whereas such micro-fillers as milled carbon fibers, while providing substantial increase in stiffness, have little effect on foam strength and toughness. Scaling models relating filled solid polymer properties to those of the filled foams have been considered and shown to have a predictive potential.

Keywords polymer foams, strength, toughness, nanoclay, carbon fibers

1. Introduction

Currently there is an increasing worldwide interest in modern technologies based on renewable raw materials. The introduction of plant components into polyurethane (PUR) systems meets all the aims of sustainable development and is an important challenge for chemical companies. Polyisocyanurates (PIRs) are synthesized using two basic components: polyols and isocyanates. In recent years, increasing interest from industry concerning polyols derived from renewable sources (different natural oils, such as rapeseed oil (RO), castor, soya, palm, sunflower oils, etc.) has been perceived. These natural ingredients can be successfully used to obtain different PIRs including porous composites. Moreover, the anticipated effects of progress in polymer materials should lead to the improvement of their properties and the reduction of their manufacturing cost. This is one of the reasons to carry on the research in the field of porous composites with the use of nano- and micro-fillers [1].

Rigid low-density closed-cell PIR foams are used primarily as a thermal insulation material in building construction and in the global appliances (refrigerators, freezers, etc.) industry, as well as in aerospace industry. Although not expected to bear load, low-density foams still have to exhibit strength and toughness adequate for loading conditions in the intended applications. Various high-stiffness nano- and microfillers such as organically modified clay, carbon nanotubes, and metal oxides [[1]-[4]], as well as carbon microfibers [[5]] have been shown to improve considerably the mechanical response of PUR and PIR foams at relatively low filler loadings. Prediction of strength of foam materials based on micromechanical considerations is complicated due to large variability in foam morphology. However, scaling relations linking foam strength and toughness to density and morphological parameters of the foams and deformability or strength characteristics of the foam struts have been derived and verified experimentally, see e.g. [[6], [7]]. The present study aims at

experimental evaluation of the effect of commercially available fillers on the strength and toughness of RO PIR foams and their relation to the strength of filled solid polymers.

2. Materials

2.1. Polyol synthesis

Polyols on the basis of renewable natural oils, suitable for obtaining PUR and/or PIR, can be obtained by different methods. Most often the esterification or epoxidation of oils is applied. In the present work, for producing of PUR, polyol obtained by amidization of RO with diethanolamine was used. Temperature: 140˚C, catalyst: zinc acetate. The RO / diethanolamine molar ratio was 2.9 / 1.0. RO obtained from the company *Iecavnieks* (Latvia) was used for the synthesis of polyols. Firstly, optimum synthesis conditions of polyols suitable for obtaining PUR were determined. The synthesis process was controlled from the diethanolamine (acid value and NH value) conversion degree. The structure of polyol was characterized from FTIR spectroscopy data.

2.2. Fillers

Four different nanoclays or organically modified montmorillonites (MMT): Cloisite® 15A, Cloisite® 30B, Cloisite® 93A (produced by *Southern Clay Products, Inc.*) and Dellite® 43B (produced by *Laviosa Chimica Mineraria S.p.A.*) were used as fillers of RO PIR foams. The clays are purified natural montmorillonites modified as follows: Cloisite® 15A is modified with a dimethyl dehydrogenated tallow quaternary ammonium having a cation exchange capacity of 125 mequiv/100 g, 30B - modified by methyl tallow bis-2-hydroxyethyl ammonium with a concentration of 90 meq/100 g clay, 93A - modified with a quaternary ammonium salt (methyl, dihydrogenated tallow ammonium) in a concentration of 90 mequiv/100 g of clay, and Dellite® 43B is modified by dimethyl benzylhydrogenated tallow ammonium. Multi-wall carbon nanotubes Nanocyl® NC7000 (produced by *Nanocyl s.a.*) with average diameter of 9.5 nm and average length of 1.5 μm (according to manufacturer's data), as well as zinc oxide nanoparticles Zano® 20 (produced by *Umicore Zinc Chemicals*) with the size of ca. 30 nm were also used for filling the foams.

Carbon-fiber-filled foams were manufactured using Tenax-A milled carbon fibers, with 7 μm diameter, of two types. Type 383 fibers had length within 50-150 μm range with the average length of 100 μm, whereas Type 385 fiber length was in the 40-70 μm range having the average length of 60 μm. The bulk density of the fibers amounted to 350 kg/m^3 and 550 kg/m^3, respectively.

2.3. Foam production

The formulations used in this study were polyols from RO, and a higher functional polyether polyol based on sorbitol Lupranol 3422 (it contains only secondary hydroxyl groups, OH Number 490 mg KOH/g) - from *BASF*. As additives, surfactant NIAX Silicone L6915LV, from *Momentive Performance Materials* and catalyst Polycat 5 from *Air Products* were used. Tris-chloropropyl phosphate (TCPP), used as a flame retardant, was supplied by *Albemarle* and as blowing agent, a

mix of water and cyclo-pentane was used. As an isocyanate, polymeric diphenylmethane diisocyanate - IsoPMDI 92140, supplied by *BASF*, was used.

PIR samples were obtained by mechanically mixing appropriate amounts of IsoPMDI 92140 and the polyol system (polyols, surfactant, catalysts, and blowing agent) for 10-15 s. The unreacted mixture was poured into a plastic mould (20 x 30 x 10 cm) for free foaming. The polymerization reaction took place at room temperature for all the obtained samples and was completed in about 3-5 min. The foam samples were conditioned before tests for at least 24 h.

Nanoclay loadings in the range of 1% to 5% by weight were considered. The exfoliation of MMT nanoclays in RO polyol was performed by MRC Ultrasonic Cell Crusher. The same procedure was applied also for mixing Zano 20 and Nanocyl NC7000 fillers in RO polyol at 1 % wt. When producing microfiber-filled foams, carbon fibers of the selected type were mixed into the polyol system. After stirring, the fiber suspension in polyol was degassed, the foaming agent added, the mixture stirred and foamed. Three different fiber loadings were obtained: 2%, 4% and 6% by weight. Good dispersion was achieved, as suggested by the change in viscosity of the filled polymer for nano- and by optical microscopy for micro-fillers. The content of different fillers in the foams was calculated on the basis of initial weights.

For characterization of the mechanical properties of solid, monolithic unfilled and nanofilled polymers, the mixture prepared as described above was poured in plastic ampoules of ca. 14 mm diameter and 80 mm length. The ampoules were subjected to centrifuging to eliminate bubbles.

3. Characterization of mechanical properties

3.1. Strength

For mechanical testing, specimens were produced from slices of the foam blocks cut along the rise direction of the foams (for illustration of the free foaming , see Fig. 1) .   The specimens for tension
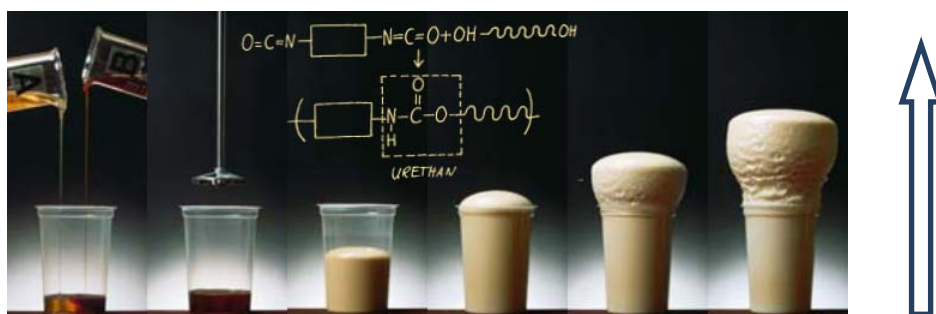

Fig. 1. Illustration of the free foaming process. The arrow shows the foam rise direction.

tests were machined to a dog-bone shape, with a rectangular test section of 85 mm length, 22 mm width, and 20 mm thickness. The specimen orientation was chosen so that the mechanical response in the direction normal to foam rise could be characterized. An extensometer with 50 mm base

length was used for strain measurement in the loading direction. For gripping, metallic plates with hooks were glued to the ends of the specimens. Tensile tests were carried out by stroke control, at a displacement rate of 8 mm/min. For compressive tests, rectangular specimens of dimensions 80 x 30 x 30 mm were cut from the foam slices and loaded at a rate of 10 %/min. Thus comparable specimen gauge length and loading rate was ensured for both, tensile and compressive tests normal to the foam rise direction. Thin Teflon films were put between the top and bottom ends of specimens and the plates of the testing machine to reduce the friction in compression tests.

Apparent density of each of the foam specimens was determined before the tests. The variation of density with filler loading is shown in Figs. 2 and 3 for MMT fillers and in Fig. 4 for carbon fiber fillers (foams with different initial densities in 34 to 50 kg/m^3 range were filled, as seen in Figs. 2-4). Note that the markers in Figs. 2 and 4 have been slightly offset with respect to the correct filler content values for better legibility. The presence of fillers apparently had larger effect on foam density when the initial, neat foam density was lower. Addition of Zano 20 at 1 % wt. increased foam density from ca. 34 for neat foams to 45 kg/m^3, whereas filling by Nanocyl at the same loading produced foams with 55 kg/m^3 density.
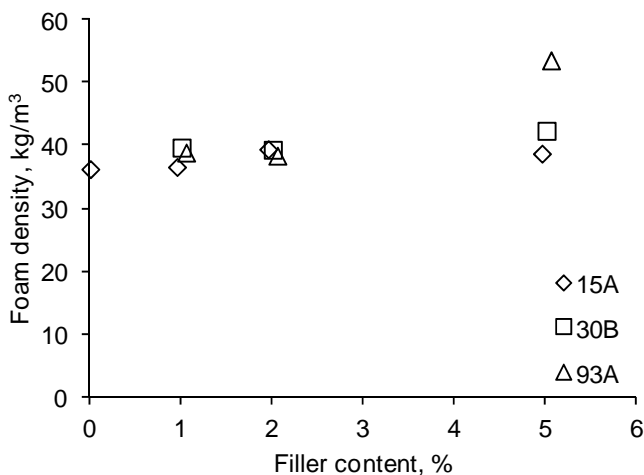
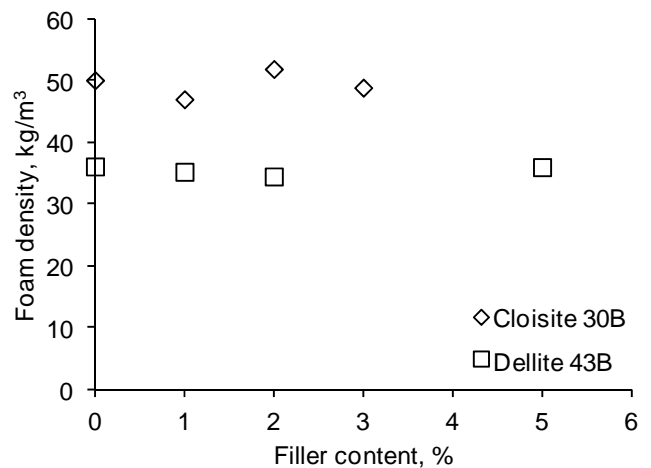Fig. 2. Foam density vs. Cloisite content
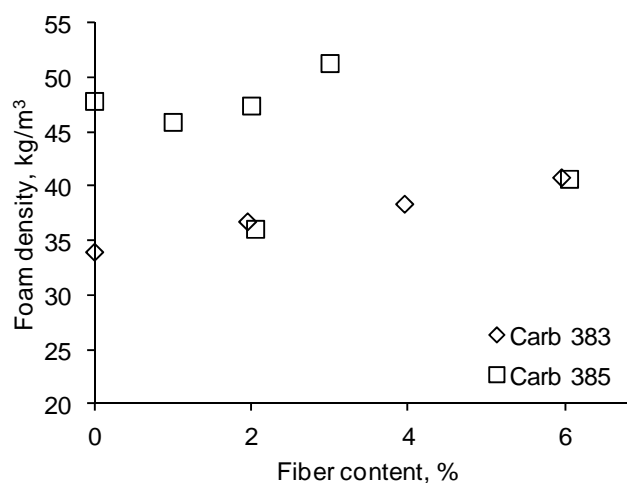
Fig. 3. Foam density vs. MMT content

Fig. 4. Foam density vs. carbon fiber content

The solid polymer samples were removed from ampoules upon setting of the polymer, and

cylindrical dog-bone shaped specimens were manufactured by turning. The length of the test section of the specimens amounted to ca. 28 mm and diameter to 5.5 mm. Specimen ends were glued into tubular aluminum tabs. Tensile tests were carried out by stroke control with the displacement rate of 1 mm/min. Young's modulus was determined from the initial, linear part of the stress-strain diagram, while the maximum stress before failure was taken as the tensile strength [[3]].

3.2. Toughness

Fracture toughness of the foams for crack propagation in mode I in the foam rise direction was determined according to ASTM Standard D5045-99. Compact tension specimens with the height and width equal to 65 mm and 20-mm thickness were used. Detailed description of the test procedure and results for neat foams is provided in [[8]].

4. Results and discussion

4.1. Strength of neat polymer foams

By varying the amount of blowing agent, rigid neat RO PIR foams with apparent density in the range from 30 to 60 kg/m^3 were obtained. The dependence of foam strength on density is shown in Fig. 5 for tensile and in Fig. 6 for compressive loading normal to the foam rise direction. It is seen in the graphs that the compressive strength appears to be slightly more affected by foam density than the tensile strength.
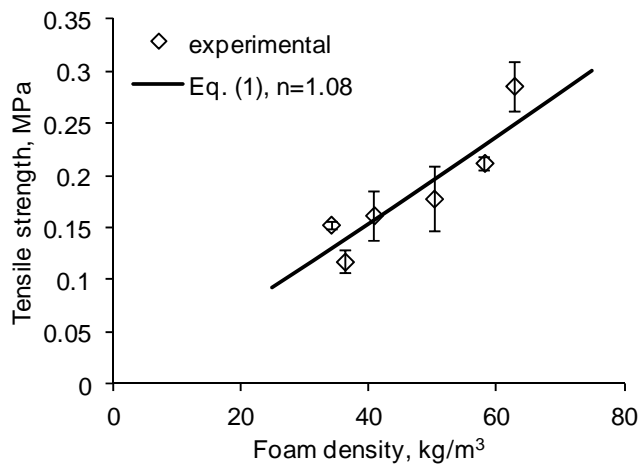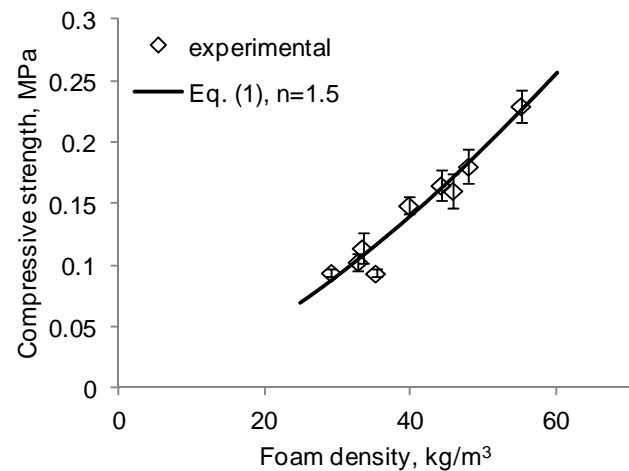

Fig. 5. Tensile strength vs. neat foam density   Fig. 6. Compressive strength vs. neat foam density

Assuming a particular geometry of foam cells, a power-low relationship for foam strength σ_f as a function of density ρ_f has been derived in [[6]]

$$\sigma_f = C\rho_f^n \tag{1}$$

where the factor C is related to properties of the cell wall material. For tensile strength of brittle foams, $C = c_8 \sigma_s / \rho_s^n$ where c_8 is a numerical prefactor, σ_s designates tensile strength of the solid cell-wall material and ρ_s - its density. Approximating the respective strength data with Eq.

(1), the value of $n = 1.08$ was obtained for tensile and $n = 1.5$ for compressive strength. The agreement of Eq. (1) with the experimental data is reasonably good as seen in Figs. 5 and 6.

4.2. Tensile strength of nanoparticle-filled polymer foams

The presence of nanofiller in a polymer may affect its mechanical characteristics as well as the density and morphology of polymer foams. The scaling relation Eq. (1) should equally apply to filled polymer foams. Hence, the tensile strength of filled polymer foams should scale with solid polymer strength as follows

$$\sigma_f\left(c_{fil}\right) = c_8\left(\frac{\rho_f\left(c_{fil}\right)}{\rho_s\left(c_{fil}\right)}\right)^n \sigma_s\left(c_{fil}\right) \tag{2}$$

where c_{fil} designates filler loading. For low filler concentrations of practical interest, its effect on density of the solid polymer can be neglected, $\rho_s\left(c_{fil}\right) \approx \rho_s(0)$, and polymer strength approximated by a linear function of filler concentration

$$\sigma_s\left(c_{fil}\right) = \sigma_s(0)\left(1 + \mu c_{fil}\right) \tag{3}$$

with μ denoting the reinforcement efficiency factor. It is convenient to introduce the reduced foam strength as follows

$$\sigma_f^*\left(c_{fil}\right) = \sigma_f\left(c_{fil}\right)\left[\rho_f(0)/\rho_f\left(c_{fil}\right)\right]^n \tag{4}$$

(Note that a similar reduction method for foam strength has been introduced in [[9]].) Then, by combining Eqs. (1) − (4), the reduced strength can be expressed via neat foam strength and filler content as follows

$$\sigma_f^*\left(c_{fil}\right) = \sigma_f(0)\left(1 + \mu c_{fil}\right) \tag{5}$$

In order to determine the reinforcement efficiency factor experimentally, the strength of neat and filled foam cell wall material, e.g. struts, should be measured. Such tests are, however, prohibitively complicated even for strut stiffness, due to small dimensions and non-uniform shape of the struts. Macroscopic samples of monolithic polymer are likely to yield only a lower bound for strut strength due to differing flaw structure, with more severe flaws likely to be introduced in polymer samples during manufacture compared to the flaws in microscopic struts arising during rise of the foams. However, μ characterizes the ratio of neat and filled strut strength as seen in Eq. (3) rather than the absolute strength values. Since the flaw distribution in neat and filled polymer samples, prepared following the same procedure, should be comparable, the difference in their strength should reflect variation in intrinsic strength due to the presence of a filler. Hence, as a first approximation, an estimate of μ can be obtained using the ratio of strength of neat and filled polymer samples.

Tensile strength of monolithic neat and filled RO PIR samples is presented in Table 1. Filler content

in the filled solid polymers amounted to 1 % wt. Solving Eq. (3) for μ, expressing c_{fil} in weight percent, and using the average strength data from Table 1, estimates of μ were obtained and presented in Table 1.

Table 1. The effect of filler at 1 wt. % on polymer strength

Filler	no filler	Zano 20	Nanocyl	Cloisite 30B	Dellite 43B
Mean strength, MPa	58.5	65.4	64.9	65.1	60.5
Standard deviation, MPa	6.1	2.7	1.5	2.9	0.7
Number of tests	10	4	4	4	3
μ, 1/%	-	0.119	0.111	0.114	0.034

The reduced tensile strength of foams as a function of nanoclay concentration is shown in Figs. 7 – 9. It is seen that the strength varies almost linearly with filler loading for low concentrations, up to 3 % wt., in qualitative agreement with Eq. (5). At the highest concentration of 5 % wt. considered, the reinforcement efficiency appears to drop, with foam strength being comparable or lower than that at 2 % wt. loading as seen in Figs. 7 and 9.

The strength of low density foams filled with three differently modified Cloisite nanoclays is shown in Fig. 7 as a function of clay loading. It is seen that the strength of all three foams appear to be quite close at the filler concentrations of 1 and 2 % wt., with overlapping scatter bands. The variation of foam strength with filler content, predicted by Eq. (5) using the value of reinforcement efficiency factor μ determined for Cloisite 30B, is in good agreement with test results for the lower fiber loadings. Reasonable agreement of Eq. (5) with strength data is seen also for higher density foams, Fig. 8. However, for low density foams filled with Dellite 43B nanoclay, Eq. (5) using the respective μ value from Table 1 appears to underpredict foam strength shown in Fig. 9.
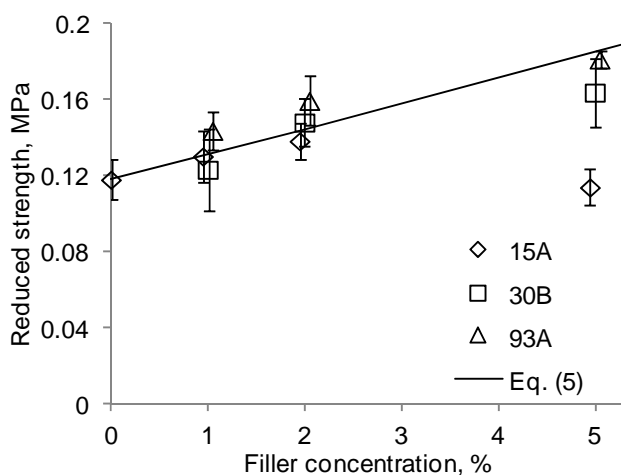

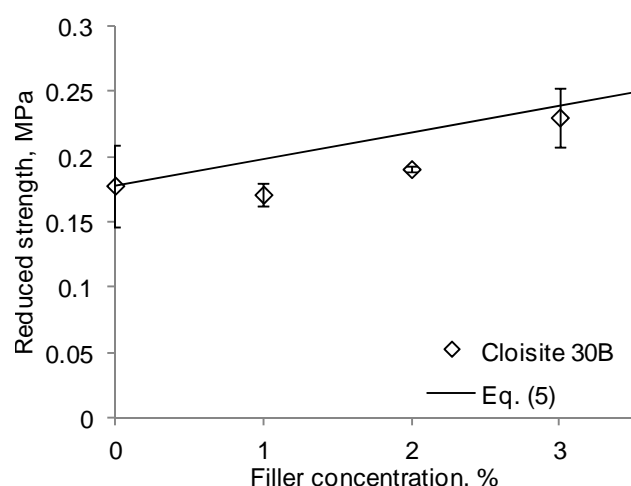Fig. 7. Reduced tensile strength as a function of nanoclay loading for three Cloisite clays

Fig. 8. Reduced tensile strength as a function of Cloisite 30B nanoclay loading

At a given filler loading, the theoretical dependence of tensile strength on foam density can be easily show to have the form

$$\sigma_f\left(c_{fil}\right) = C\rho_f^n\left(1 + \mu c_{fil}\right) \tag{6}$$

with the parameter C and n values as determined for neat foams. It is seen in Table 1 that the μ values for ZnO, carbon nanotube, and Cloisite 30B filled polymers are very close, with the average of $\mu = 0.114$. The strength of foams with the fillers mentioned above at 1% wt. is plotted as a function of the filled foam density in Fig. 10. A reasonable agreement with the prediction by Eq. (6) using the average μ value is seen.
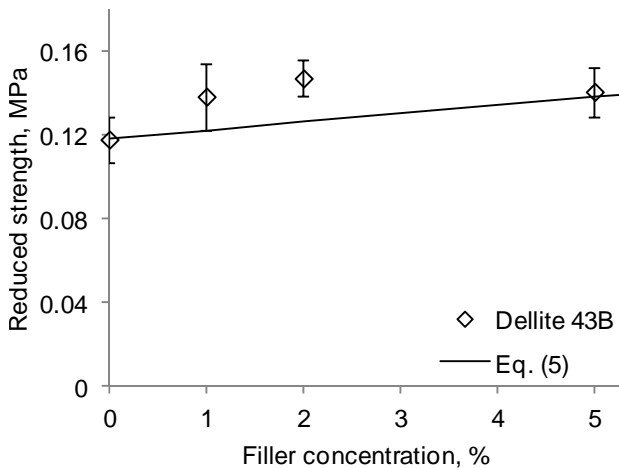
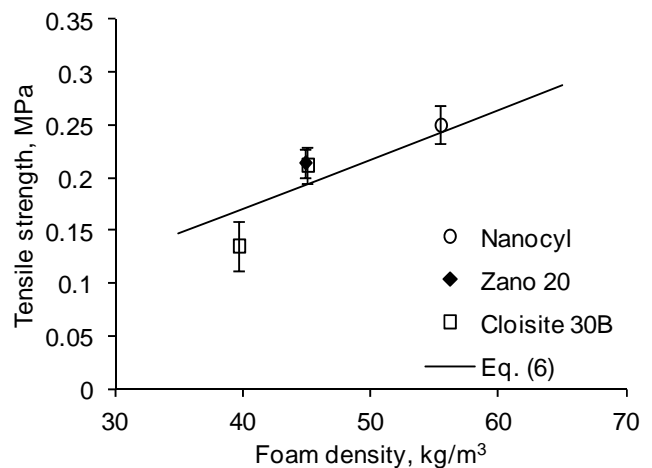Fig. 9. Reduced tensile strength as a function of Dellite 43B nanoclay loading

Fig. 10. Tensile strength vs. foam density of filled foams containing 1 % wt. of nanoparticles

4.3. Strength of carbon fiber-filled polymer foams

The reduced tensile strength of foams filled with milled carbon fibers is shown in Fig. 11 as a function of filler content. No apparent effect on the strength is observed for either of the fiber types differing in average length by a factor of ca. 1.7. The reduced compressive strength of foams with two different densities, shown in Fig. 12, was also barely affected by the presence of fiber filler. For ease of comparison, the strength of unfilled foams is indicted by dashed lines in Figs. 11 and 12.
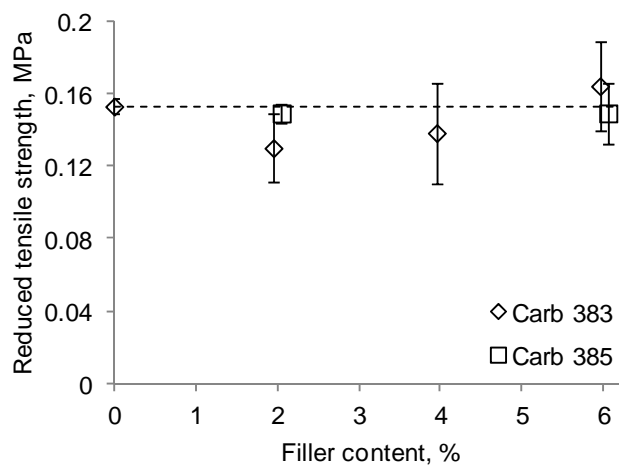
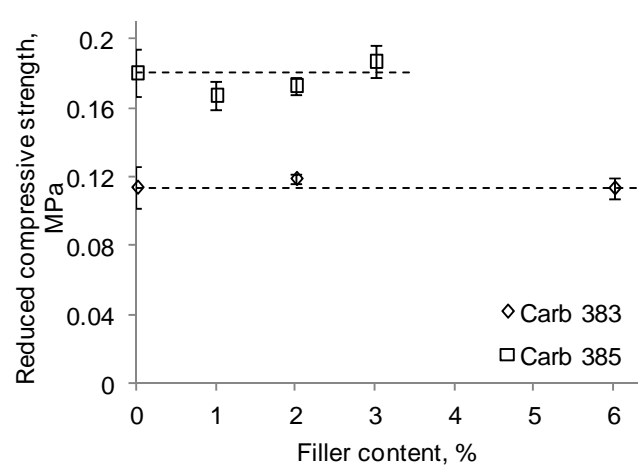Fig. 11. Reduced tensile strength vs. carbon fiber content

Fig. 12. Reduced compressive strength vs. carbon fiber content

SEM and optical microscopy revealed that the carbon fibers were located within the cell wall

material, in cell struts and nodes, which resulted in appreciable increase in foam stiffness [[5], [10]]. However, polymer struts containing no fibers were also observed even at the highest fiber loading, which might have served as the sites of failure initiation, thus negating any increase in strength of the fiber-reinforced struts.

4.4. Fracture toughness of filled polymer foams

For the range of RO PIR foam density considered, mode I fracture toughness for crack propagation along the foam rise direction was found to vary approximately linearly with foam density [[8]]

$$K_{Icf} = C_k \rho_f \tag{7}$$

Relation Eq. (7) is plotted in Fig. 13 by a solid line together with the experimental toughness values of foams with nano- and microfillers at 1 wt. % loading. It is seen that the presence of carbon microfibers apparently fails to enhance foam resistance to cracking, since the toughness of carbon 385 fiber filled foams agrees within experimental scatter with that of neat foams of comparable density.
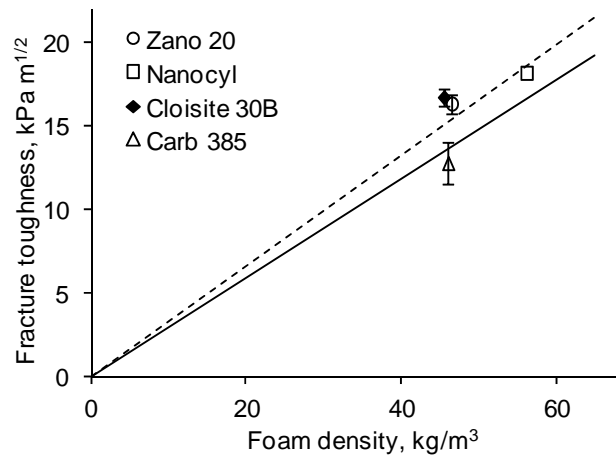

Fig. 13. Fracture toughness of filled foams at 1 wt. % loading. Solid line corresponds to neat foam toughness, dashed line plots prediction by Eq. (9)

Scaling relations derived in [[6], [7]] for foam toughness have the form

$$K_{Icf} = C_k \rho_f^n \tag{8}$$

where $C_k \sim \sigma_s \sqrt{l_s} / \rho_s^n$ with l_s designating strut length and the exponent estimates ranging from n = 1 [[7]] to 1.5 [[6]]. Combining Eqs. (3), (7), and (8) (with n = 1), we obtain for filled foam toughness

$$K_{Icf}(c_{fil}) = C_k \rho_f (1 + \mu c_{fil}) \tag{9}$$

with the parameter C_k value as determined for neat foams. The prediction according to Eq. (9) is plotted in Fig. 13 by dashed line, using the average μ value for ZnO, carbon nanotube, and Cloisite 30B filled polymers. It is seen that Eq. (9) reasonably accurately reflects the observed increase of

nanofilled foam toughness with respect to that of neat foams. However, the strut length factor, neglected in Eqs. (7) and (9), should be explicitly incorporated in the toughness relations since the variation of strut length with foam density may differ for neat and filled foams.

5. Conclusions

Production technology of rigid low-density polyisocyanurate foams obtained from renewable resources, with the polyol system comprising up to 80% of rapeseed oil-derived esters, has been developed. The production process is energy-saving and environmental friendly. The effect of nano-scale (organically modified MMTs, carbon nanotubes, ZnO particles) and micro-scale (milled carbon fibers) fillers on the strength and toughness of RO PIR foams has been experimentally evaluated. Taking into account the increase in foam density due to the presence of filler, carbon microfibers yielded negligible effect on the tensile and compressive strength and fracture toughness of foams in the 2 to 6 % wt. loadings studied. By contrast, nanofillers at 1 to 3 % wt. loading increased both strength and toughness of the foams. The reinforcement efficiency of the nanofillers can be roughly estimated by strength tests of filled solid polymers.

References
[1] M. Kuranska, A. Prociak, M. Kirpluks, U. Cabulis, Porous polyurethane composites based on bio-components. Compos Sci and Techn 75 (2013) 70–76.

[2] Ł. Piszczyk, M. Strankowski, M. Danowska, J.T. Haponiuk, M. Gazda, Preparation and characterization of rigid polyurethane–polyglycerol nanocomposite foams. Eur Polym J 48 (2012) 1726–1733.

[3] M.C. Saha, Md.E. Kabir, S. Jeelani, Enhancement in thermal and mechanical properties of polyurethane foam infused with nanoparticles. Mater Sci Eng A 479 (2008) 213–222.

[4] M.C. Saha, Md.E. Kabir, S. Jeelani, Effect of nanoparticles on mode-I fracture toughness of polyurethane foams, Polym Compos 30 (2009) 1058-1064.

[5] V. Yakushin, U. Stirna, L. Bel'kova, L. Deme, I. Sevastyanova, Properties of rigid polyurethane foams filled with milled carbon fibers. Mech Compos Mater 46 (2011) 679- 688.

[6] M.F. Ashby, The mechanical properties of cellular solids. Metall Trans A, 14 (1983) 1755-1769.

[7] J.B. Choi, R.S. Lakes, Fracture toughness of re-entrant foam materials with a negative Poisson's ratio: experiment and analysis. Int J Fract 80 (1996) 73-83.

[8] J. Andersons, E. Spārniņš, U. Cābulis, U. Stirna, Fracture toughness of PIR foams produced from renewable resources. Key Eng Mater 525-526 (2013) 29-32.

[9] M.C. Hawkins, B. O'Toole, D. Jackovich, Cell morphology and mechanical properties of rigid polyurethane foam. J Cell Plast, 41 (2005) 267-285.

[10] J. Andersons, J. Modniks, U. Cābulis, U. Stirna, Modeling the effect of short-fiber filler on the stiffness of polyisocyanurate foams, in: D.T. Tsahalis (Ed.), Proc. of 5th IC-SCCE, Vol. II, 2012, pp. 343- 348.